

Structural characterisation of (11 $\bar{2}$ 0) 4H-SiC substrates by cathodoluminescence and X-ray topography

P. Hidalgo^{1,2,a}, L. Ottaviani¹, H. Idrissi¹, M. Lancin¹, S. Martinuzzi¹, and B. Pichaud¹

¹ Laboratoire TECSEN, UMR 6122, Université de Marseille St Jérôme case 231, 13397 Marseille, Cedex 20, France

² Dpto. Física de Materiales, Fac. Ciencias Físicas - UCM. Ciudad Universitaria, 28040 Madrid, Spain

Received: 2 July 2003 / Accepted: 9 December 2003 – © EDP Sciences

Abstract. Silicon Carbide (SiC) is a wide band gap semiconductor, having opto-electronic properties that are suitable for many applications. Some structural defects due to crystal growth and/or doping technologies are commonly present in the substrates of SiC. The (11 $\bar{2}$ 0)-oriented 4H-SiC bulk wafers are particularly investigated, due to some advantages with respect to the (0001)-Si face. One of these advantages is a better crystal reordering during post-implantation annealing. In this paper cathodoluminescence (CL) and X-Ray topography measurements have been carried out in order to investigate the optical and structural properties of commercial (11 $\bar{2}$ 0) 4H n^+ -type substrates.

PACS. 61.72.Ff Direct observation of dislocations and other defects (etch pits, decoration, electron microscopy, x-ray topography, etc.) – 61.72.-y Defects and impurities in crystals; microstructure – 78.60.Hk Cathodoluminescence, ionoluminescence

1 Introduction

Silicon Carbide (SiC) is a wide band-gap semiconductor, having opto-electronic properties that are suitable for many applications, especially high power and high frequency devices. Some structural defects due to crystal growth, are commonly present in the substrates of SiC. One of the most important technique to grow this semiconductor is the Lely-modified technique [1,2]. A lot of efforts have been carried out in order to control the formation of structural defects in the modified Lely process and to investigate the influence of such defects on the electrical properties.

As the impurity diffusivities in SiC are very low, implantation of dopants is one of the most important way to produce homojunctions in this material. A post-implantation annealing is necessary in order to reduce the implantation damage, aiming at recrystallizing the implanted zone, however, other polytype crystals could be induced. Normally to prevent the formation of polytypes, implantations are processed at elevated temperatures, but a low temperature processing is desired in order to reduce the contamination from ambient.

(1 $\bar{1}$ 00)-oriented 4H SiC is known to preserve the polytype structure of implanted layer due to that the polytype of the growth crystal in this direction depends on the polytype of the seed, but that is not the case of the (0001)-oriented SiC [3]. Moreover, (11 $\bar{2}$ 0)-oriented SiC face is mainly studied today due to fewer negative charges at the 4H-SiC MOS interface than at the (0001)-oriented 4H-

SiC face [4], leading to better channel mobilities and lower threshold voltages measured on planar MOSFET's [5,6].

2 Experimental setup

For this work a (11 $\bar{2}$ 0)-oriented 4H-SiC commercial wafer cut from an (0001)-oriented ingot with both faces polished, was investigated. Samples are n^+ -type ($5.0 \times 10^{18} \text{ cm}^{-3}$) with a thickness of 216 μm .

Structural properties of samples were investigated by X-ray topography technique (XRT). X-ray topographs were registered in Lang transmission geometry with $\text{AgK}\alpha$ wavelength.

In order to investigate the optical properties, CL measurements were performed in a Hitachi S-2500 scanning electron microscope, equipped with a computer controller Oriol 7720 monochromator and a Hamamatsu R928 photomultiplier for detection. The spectral resolution was better than 1 nm. The microscope is equipped with a temperature controller system that permits CL measurements from 77 K. Details of the experimental setup for spectral and panchromatic CL measurements are presented elsewhere [7].

3 Results

Figure 1 shows a typical CL spectrum recorded on (11 $\bar{2}$ 0)-oriented 4H SiC sample with an accelerating voltage of

^a e-mail: phidalgo@fis.ucm.es

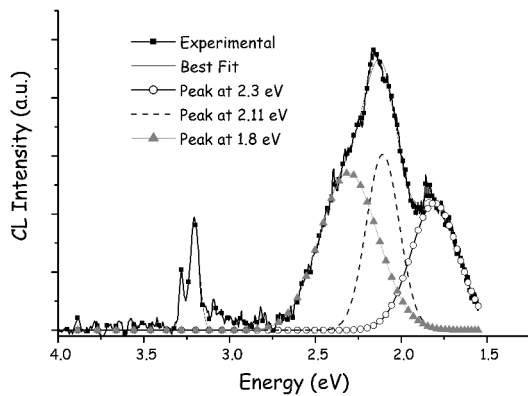


Fig. 1. Typical CL spectrum of (11-20)-oriented n^+ -type SiC. Deconvolution of the broad band centred around 2 eV shows three emissions at 2.3 eV, 2.11 eV and 1.8 eV respectively.

25 kV and at 77 K. It is possible to identify three emissions in this spectrum. First one corresponds to band to band transition centered at 3.28 eV, second one centered at 3.2 eV corresponding to an excitonic transition and finally a broad band known as green band (GB) and centered around 2 eV.

It is clear that in the GB observed in the CL spectrum, at least three different radiative centers are involved. The deconvolution of this broad band in Gaussian peaks permit to identify these three components (Figure 1): one centered at 2.3 eV, one centered at 2.11 eV and another one centered at 1.8 eV. In Recent studies of CL carried out in (0001)-oriented 4H n-type SiC samples, it is possible to observe the emissions centered at 2.3 eV and 2.11 eV but not the emission centered at 1.8 eV. In a previous work we have attributed this last peak to recombination of carriers at centres associated to dislocations in the basal plane [8]. The corresponding energies at 2.3 eV and 2.11 eV prove the existence of at least two deep levels that some authors attribute to boron on carbon sites and/or to complexes involving boron atoms and vacancy clusters [9]. If the beam is defocused in order to reduce the excitation level, a very high increment of the luminescence signal is observed accompanied with a change in the spectrum as is shown in Figure 2. Both emissions related to band gap transitions disappear and only the GB emission is observed with a very high intensity.

It is clear from Figures 1 and 2 that emission intensities in the sample depend on the excitation conditions. Different spectra were recorded at different energies of the electron beam, first with a focused beam and then with a defocused beam for each accelerating voltage. Integrated CL intensity signals for focused and defocused beam are shown in Figure 3. It is clear that in both cases, CL signal increases when the potential increases but when high excitation conditions are used (high accelerating voltages) a saturation of radiative centers is observed. It is also possible to observe in Figure 3, that luminescence depends on excitation density for the same beam energy. A lower excitation energy (defocused beam) produces a higher lu-

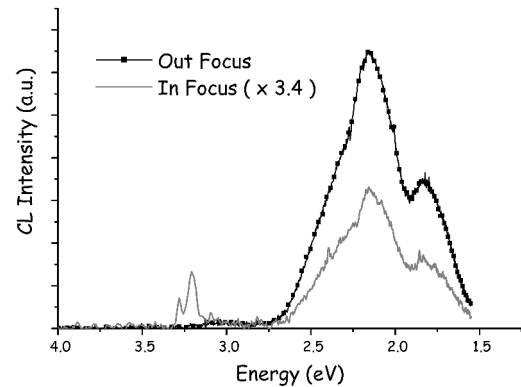


Fig. 2. CL spectra recorded at 77 K and with different excitation conditions.

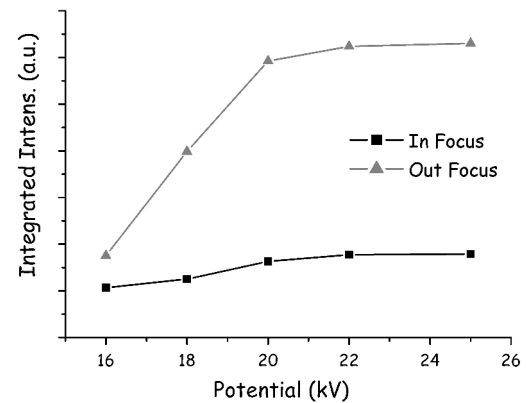


Fig. 3. CL intensity at 77 K as function of energy of the beam. A high reduction of intensity is observed when electron energy is reduced.

minescence: this effect is normally associated to a competitive mechanism between non-radiative and radiative recombination processes. When the energy of the beam is reduced this difference between focused and defocused beam, decreases.

From spectra recorded in the sample, it is clear that the most important emission is the green band. We have investigated the evolution of the emissions involved in this broad band with temperature in order to know if a modification in the emission rate of the radiative centers is observed when the temperature change. To do that the temperature was increased from 80 K to 200 K and the intensity of the different emissions involved in GB were compared (Figure 4). From Figure 4 it is clear that when the temperature increases the total intensity of GB decreases. Another result is that when the temperature increases, the intensity of bands centered at 2.3 eV and 1.8 eV does not change but the intensity of the emission band centered at 2.11 eV decreases.

After CL investigations X-ray topography measurements were recorded. X-ray topographs show the strain fields developed around three kinds of structural defects (Figure 5a). In Figure 5b screw dislocations with Burger vector ($\mathbf{b} = c$ along [0001]) are observed. The density of

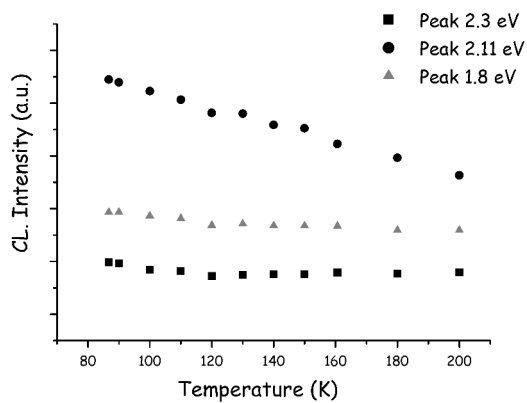


Fig. 4. CL intensities of emissions involved in the broad band centered around 2 eV as function of the temperature.

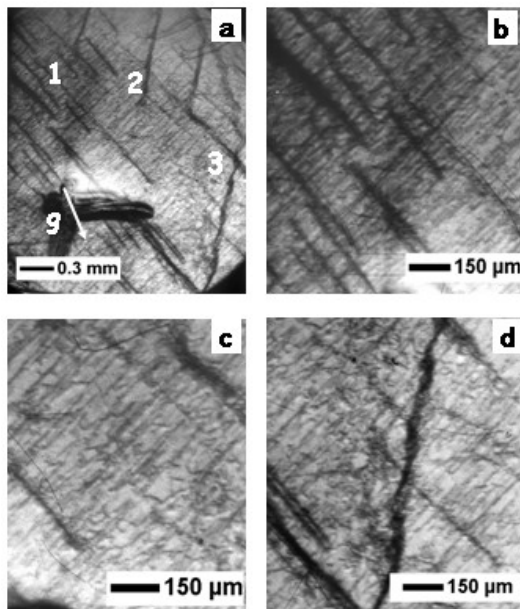


Fig. 5. X-ray topographies recorded in (11 $\bar{2}$ 0)-oriented 4H-SiC sample. (a) General image, (b) detail of region 1 showing screw dislocations, (c) detail of region 2 showing perfect or partial dislocations on the basal plane and (d) low angle boundary.

this type of defects in the sample is around $7 \times 10^2 \text{ cm}^{-2}$. In Figure 5c other types of defects are observed, they are in this case perfect or partial dislocations on the basal plane ($\mathbf{b} = 1/3 \langle 11\bar{2}0 \rangle$) with a density of $9 \times 10^3 \text{ cm}^{-2}$. And finally the third type of defects are observed in Figure 5d. In this case defects correspond to low angle boundaries. It is always necessary to keep in mind that information from

Lang transmission geometry comes from an integration of the entire volume.

4 Conclusions

In conclusion, (11 $\bar{2}$ 0)-oriented 4H SiC n-type was investigated. CL spectra show three main emissions, the band gap emission, the exciton related emissions and a broad band, known as GB, centered around 2 eV and formed by different components. A study of the behavior of these three emissions which are involved in the GB with temperature show that only the radiative center with an energy of 2.11 eV is affected by temperature in the range of 77–200 K. The other two radiative emissions remain constant in intensity when temperature increases. It is observed that CL intensity is higher when excitation intensity is lower. In the case of low excitation density, no emissions related to band-to-band transitions are observed and only the GB with a high intensity is observed.

X-ray topography show three different types of defects in the sample, screw dislocations and perfect or partial dislocations on basal plane, both with a very high density, and low angle boundaries.

References

1. Y. M. Tairov, V. F. Tsvetkov, *J. Cryst. Growth* **43**, 209 (1978)
2. D. L. Barrett, R. G. Seidensticker, W. Gaida, R. H. Hopkins, W. J. Choyke, *J. Cryst. Growth* **109**, 17 (1991)
3. M. Satoh, K. Okamoto, Y. Nakaike, K. Kuriyama, M. Kanaya, N. Ohtani, *Nucl. Instrum. Methods Phys. Res. B* **148**, 567 (1999)
4. H. Yano, T. Kimoto, H. Matsunami, *Mater. Sci. For.* **353**, 627 (2001)
5. H. Yano, T. Hirato, T. Kimoto, H. Matsunami, *IEEE Electron Device Lett.* **20**, 611 (1999)
6. K. Kojima, T. Ohno, T. Fujimoto, M. Katsuno, N. Ohtani, J. Nishio, T. Suzuki, T. Tanaka, *Appl. Phys. Lett.* **81**, 2974 (2002)
7. P. Hidalgo, B. Mendez, P. S. Dutta, J. Piqueras, E. Dieguez, *Phys. Rev. B* **57**, 6479 (1998)
8. L. Ottaviani, P. Hidalgo, H. Idrissi, M. Lancin, S. Martinuzzi, B. Pichaud, *J. Phys. Cond. Matter* **16**, 5107 (2004)
9. A. Kakanakova-Georgieva, R. Yakimova, A. Henry, M. K. Linnarsson, M. Syväjärvi, E. Janzen, *J. Appl. Phys.* **91**, 2890 (2002)